A Computational Study of the Stereoselective Decarboxylation in the Synthesis of Naproxen

Markus Drees,[a] Lillian Kleiber,[a] Martin Weimer,[a] and Thomas Strassner*[a]

Keywords: Asymmetric synthesis / Decarboxylation / Mechanism / Quantum-chemical calculations

The antiinflammatory drug Naproxen has been synthesized via several enantioselective routes. The recently published synthesis involving the asymmetric decarboxylation of 2-cyano-2-(6-methoxy-naphth-2-yl)propionic acid (H. Brunner, P. Schmidt, *Eur. J. Org. Chem.* **2000**, 2119) was investigated by quantum-chemical calculations. It was found that the stereochemistry of the products was determined by a concerted protonation/decarboxylation reaction. According to quantum-chemical gas-phase calculations, C–H···O and N–H···O interactions between the chiral base and the substrate in the transition state stabilize the (*S*) enantiomer by 3.7 kcal/mol. The postulated planar ketenimine anion intermediate could be ruled out on the basis of B3LYP/6-31G(d) calculations.

Introduction

Non-steroidal antiinflammatory drugs (NSAID) such as Naproxen [(*S*)-2-(6-methoxynaphth-2-yl)propionic acid; Figure 1a] or Ibuprofen (Figure 1b) are of considerable interest.[1] The demand for Naproxen increased significantly after its FDA approval as an OTC drug in 1994, which has resulted in new efforts to improve the known syntheses or to find new, more economic ones.

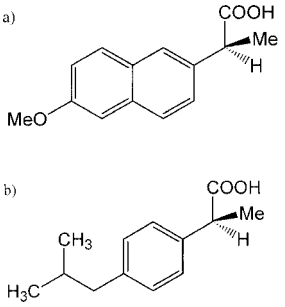

Figure 1. Examples of NSAIDs: a) Naproxen; b) Ibuprofen

Several strategies for the enantioselective synthesis have been used to date.[2–7] Noyori has very recently received the Nobel prize for his asymmetric hydrogenation reactions, also used in the synthesis of Naproxen.[8,9] Another approach was the synthesis by Larsen et al.[10] at Merck (Merck Process, Scheme 1). Starting from a racemic mixture they achieved up to 99.5% *ee* through a stereospecific addition of chiral alcohols to a ketene intermediate, separating the racemic mixture. This reaction has recently been investigated computationally and it was found that the key feature was the "concertedness" of the reaction between base, chiral alcohol, and ketene, forming a termolecular complex in the gas phase. The rate-determining step was the nucleophilic addition to the ketene carbonyl group, assisted by the deprotonation of the alcohol by the base. A stabilizing C–H···O hydrogen bond plays an important role in the transition states of this reaction.[11]

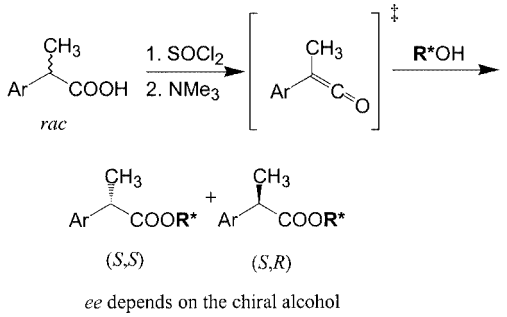

Scheme 1. Merck process

Yet another synthesis has been published by Brunner and Schmidt[12,13] (Scheme 2). The key compound was the 2-cyano-2-(6-methoxynaphth-2-yl)propionic acid (**3**), prepared by literature procedures from the readily available 2-methoxynaphthalene (**1**) by iodination to give 2-iodo-6-methoxynaphthalene (**2**) and coupling under basic conditions. The stereochemistry was set in the subsequent step, a decarboxylation in the presence of a chiral base. Hydrolysis of the nitrile finally afforded Naproxen, (*S*)-**4**, and (*R*)-**4**.

The chiral bases used in the decarboxylation step all had the same backbone, shown in Figure 2a. The best result

[a] Anorganisch-chemisches Institut, Technische Universität München,
Lichtenbergstr. 4, 85747 Garching bei München, Germany
Fax: (internat.) + 49-(0)89/289-13473
E-mail: Thomas.Strassner@ch.tum.de

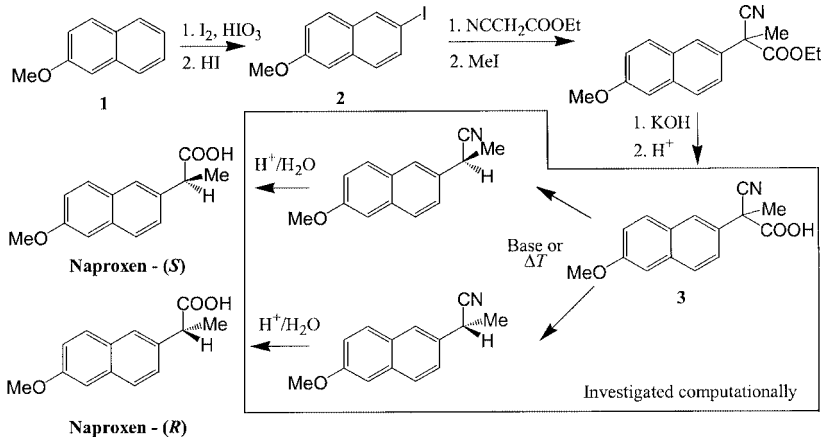

Scheme 2. Enantioselective decarboxylation pathway

(70% *ee*) for an (*S*) enantiomer was obtained with the ethoxyphenyl substituent R (Figure 2b). Experimental investigations and the calculated nuclear charges both indicated that the reaction center in the reprotonation step was the tertiary amine in the quinuclidine part of the chiral base.

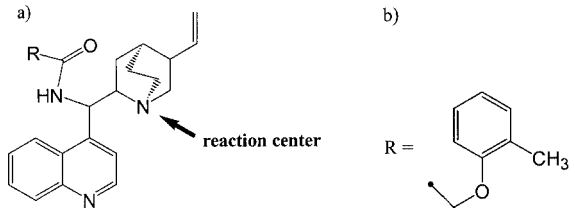

Figure 2. The chiral base that yielded the highest *ee* out of the 30 bases screened[12]

To explain the optical induction, Brunner suggested that a planar ketenimine anion was created as a prochiral intermediate, and that this could be attacked from the *Re* and *Si* faces.[12,13] In the presence of an optically active base, induction could be seen from the resulting *ee* values. The reprotonation of the anion was discussed as the step in which discrimination between the two sides was effected by the base.[12] The cinchona ligands are well known for their ability to induce chirality and are certainly able to distinguish between the enantiotopic sites of a molecule,[14–16] but the mechanism by which they induce chirality is questionable. The thermal reaction without a base yielded a racemic mixture.

In contrast with the mechanism described above, which could be termed a two-step mechanism (loss of CO_2 and reprotonation), there is also the possibility of a concerted mechanism, with the loss of carbon dioxide being induced by the reprotonation and happening simultaneously in a one-step mechanism.

Here we report quantum-chemical calculations on both pathways, that suggested by Brunner (DFT) and the concerted pathway (AM1 and DFT).

Computational Details

The density functional/Hartree–Fock hybrid model Becke3LYP[17–19] as implemented in GAUSSIAN-98[20] was used throughout this study, together with the split valence double-ζ (DZ) 6-31G* basis set (BS1) and the triple-ζ (TZ) 6-311+G** basis set (BS2). Semiempirical calculations were carried out with the Austin Model 1 (AM1)[21] as implemented in GAUSSIAN-98.[20] All geometries were fully optimized, and frequency calculations ensured that they corresponded either to minima (NIMAG 0) or to transition states (NIMAG 1) on the potential energy surface (PES). All values are unscaled, and the energies are reported in kcal/mol.

The alkaloids used as bases were too large to search the PES with DFT methods, so we chose to model the base with $N(CH_3)_3$ for the DFT calculations and to use AM1 for geometry optimizations on the full system, followed by DFT single-points for the energy evaluation. Solvation effects were calculated by use of the Onsager model[22–27] for tetrahydrofuran as implemented in GAUSSIAN-98.

Results and Discussion

The decarboxylation of the anion of **3**, giving rise to the planar ketenimine anion, was studied by calculations in which the distance between C(1) and C(2) (Figure 3) was varied between 1.7 Å and infinity (modeled by 10.0 Å).

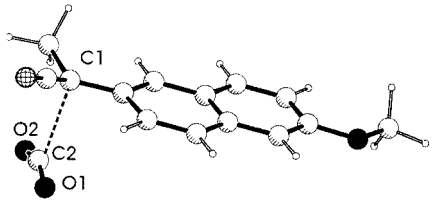

Figure 3. Decarboxylation step

Table 1. Decarboxylation reaction coordinate (BS1: B3LYP/6-31G*; BS2: B3LYP/6-311+G**)

Bond [Å] C(1)−C(2)	Angle [°] O(1)−C(2)−O(2)	ΔH (BS1) [kcal/mol]	ΔH (BS2//BS1) [kcal/mol]	ΔG_{solv} (BS1) [kcal/mol]
1.70	134.3	0.0	0.0	0.0
1.80	136.7	+0.4		+1.9
2.00	142.2	+2.2		+9.1
2.20	148.2	+3.5		+12.0
2.40	154.9	+3.9		+13.7
TS: 2.42	155.5	+3.9	+4.0	+13.8
2.60	162.0	+3.7		+14.1
2.80	168.0	+3.1		+13.9
3.00	172.2	+2.8		+14.0
π complex: 3.10	173.6	+2.7	+1.9	+14.8
3.20	174.7	+2.8		+14.6
3.40	176.1	+3.0		+14.9
10.0	180.0	+6.3	+4.2	+13.2

The energy profile for the loss of CO_2 and the change in the carbon dioxide angle O(1)−C(2)−O(2) are shown in Table 1.

The optimized geometry with a bond length of 1.7 Å was chosen as the starting point (Figure 3). The geometries were fully optimized at the B3LYP/6-31G* (BS1) level of theory; only the distance between C(1) and C(2) was constrained to the values given in Table 1. For the TS and the π complex, no constraint was used (confirmed by a frequency and IRC calculation). As can be seen from Table 1, the loss of CO_2 followed the classic profile, with the energy increasing when the bond was elongated and reaching a maximum in the transition state at 2.42 Å. An intermediate π complex could be found at 3.10 Å, where the interaction of the CO_2 molecule with the anion could clearly be seen from the O(1)−C(2)−O(2) angle of 173.6°. B3LYP/6-311+G** (BS2) geometry optimizations resulted in a transition state with an enthalpy of +3.7 kcal/mol and a C(1)−C(2) distance of 2.34 Å, the π complex had a C(1)−C(2) distance of 3.20 Å and an enthalpy of 1.5 kcal/mol.

The overall reaction profile in the gas phase was endothermic, the energy increasing when the CO_2 molecule was separated. At a distance of 10 Å the carbon dioxide was linear, the energy being calculated as +6.3 kcal/mol. The profile was independent of the basis set used. Calculations with BS2 instead of BS1 showed a similar profile, although the enthalpy of the model system with a C(1)−C(2) distance of 10.0 Å was less endothermic at +4.2 kcal/mol.

Solvent calculations (THF) with the Onsager method[22−27] for the same geometries showed that the solvated decarboxylation was even more endothermic than the gas-phase reaction. For the separated model geometry, a free energy of +13.2 kcal/mol was calculated. The energy profile of the solvated decarboxylation (Table 1) was shifted relative to the gas-phase counterpart. The free energy increased up to a point near the transition state with a local maximum of +14.1 kcal/mol. At the geometry of the separated molecules it decreased to the value of +13.2 kcal/mol mentioned above (Table 1).

The second step of the mechanism, which according to Brunner determines the stereochemistry, was the proton transfer from the base to the anionic intermediate, modeled by the planar anion and a trimethylammonium cation (Figure 4). The distance between the nitrogen center N(1) in the $HN(CH_3)_3^+$ cation and C(1) was fixed to 2.7 Å, approximately the sum of the two individual bond lengths. The distance between N(1) and the hydrogen atom H(1) transferred from the nitrogen center N(1) to the planar anion was varied, the results are shown in Table 2.

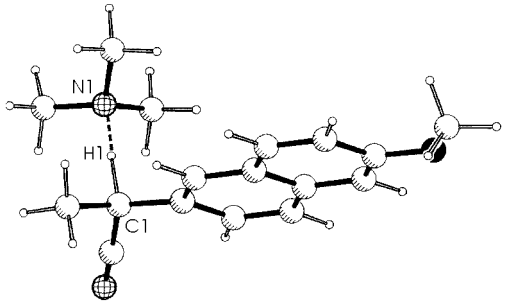

Figure 4. Reprotonation step

Table 2. Reprotonation coordinate data (BS1: B3LYP/6-31G*)

Distance [Å] N(1)−H(1)	Distance [Å] H(1)−C(1)	ΔH (BS1) [kcal/mol]	ΔG_{solv} (BS1) [kcal/mol]
1.03	1.77	+23.4	+18.6
1.10	1.65	+20.0	+16.1
1.20	1.51	+16.9	+14.1
1.30	1.40	+13.3	+15.5
1.40	1.30	+8.5	+7.8
1.50	1.20	+3.8	+3.8
1.624	1.11	0.0	0.0

The gas-phase calculation showed the expected result. The charge-separated complex was very unfavorable. The trimethylammonium ion, with an N−H bond length of 1.03

Å, and the ketenimine anion were about 23 kcal/mol higher in energy than the $N(CH_3)_3$/Naproxen product. The solvent calculation results were similar, the free energy dropped from 18.6 kcal/mol (compared to 23.4 kcal/mol in the gas phase) to 0.0 kcal/mol.

The energy penalty imposed on the molecule when the hydrogen was first transferred from **3** to the base, creating the anionic intermediate, was calculated as 112.5 kcal/mol in the gas phase. Solvent calculations with the Onsager model[22−27] for THF showed that this energy dropped dramatically to +34.1 kcal/mol for the initial proton transfer and the decarboxylation step. Together with the exothermic reprotonation step (−43.9 kcal/mol), an overall reaction enthalpy of −9.7 kcal/mol was predicted by solvent calculations. This suggests that the mechanism proposed by Brunner is energetically not favored, though not impossible.

The concerted reaction pathway was investigated by AM1[21] and DFT single-point calculations. A large molecule such as the base used here can have many conformations, resulting in a large number of local minima along the PES. To reduce this problem, we chose the approach in which the complex between base and Naproxen derivative **3** was built up step by step.[28]

The fully optimized transition states giving rise to the (*R*) and (*S*) enantiomers are shown in Figures 5 and 6, and the data on bond lengths and energies are given in Tables 3 and 4.

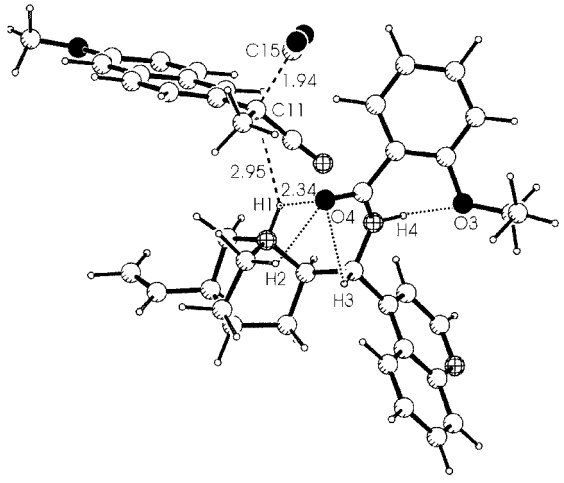

Figure 5. Transition-state (*S*) enantiomer

The calculated activation enthalpy for the TS giving rise to the (*S*) enantiomer was 4.5 kcal/mol (AM1) or 3.7 kcal/mol (DFT) lower than that relating to the corresponding (*R*) enantiomer, in agreement with the experimental result. Analogously with the results for the Merck process, C−H···O and N−H···O interactions played important roles in the transition states of the decarboxylation reaction. For the (*S*) transition state, three stabilizing interactions between the amide oxygen atom O(4) and hydrogen atoms could be found. While H(2) in the quinuclidine component and H(3) at the connection to the quinoline part of the base provided similar interactions in both transition states, the

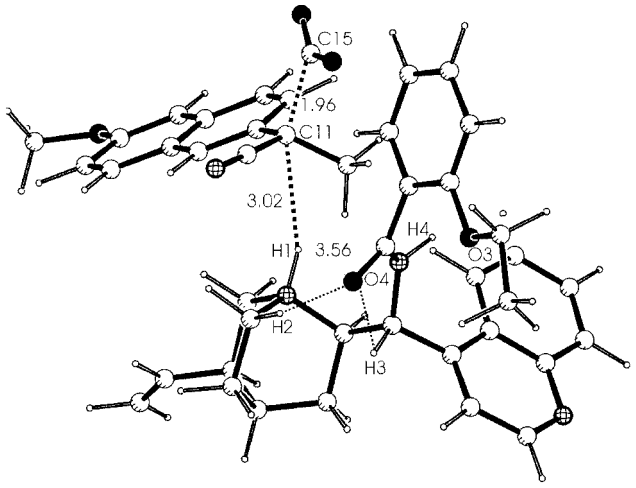

Figure 6. Transition-state (*R*) enantiomer

H(1)−O(4) distance differed significantly (Table 4). The distance of 3.04 Å in the (*R*) enantiomer prohibited significant interaction, whereas the 2.34 Å to H(1) in the (*S*) enantiomer allowed it. This could also be seen in the structure, as it created steric effects, with the Naproxen methyl group and the ethoxyphenyl ring of the base in close proximity. This steric repulsion resulted in a longer O(4)−H(1) distance and in the energy difference between the two transition states. For the ethoxy group (Figure 2b), which experimentally gave the best asymmetric induction of all screened bases, we observed another hydrogen bond between H(4) and O(3), stabilizing the (*S*) enantiomer over the (*R*) enantiomer. At 2.46 Å, it was set up for interaction in the (*S*) form, while in the (*R*) transition state the distance was too long (3.92 Å). This also provided additional stabilization for the (*S*) transition state.

IRCs starting from both transition states were carried out at the semiempiric AM1 level of theory. Figure 7 shows a part of the energy profile for the (*S*) enantiomer and the converging distances between C(11)/C(15) and C(11)/H(1) along the reaction coordinate, nicely demonstrating the concertedness of the reaction. As the distance of the CO_2 increases, the hydrogen distance to the prochiral carbon atom decreases constantly. The negative IRC coordinates point in the direction towards the starting materials, and the positive values in the other direction towards the products.

The IRC giving rise to the (*R*) enantiomer looks identical. The two bond lengths converge in a similar way, showing the same behavior and almost the same values, with the exception of the calculated enthalpy, which is 3.7 kcal/mol higher.

It is obvious that these two transition states belong to a concerted reaction, in which the energy reaches a maximum at the transition state. The loss of CO_2 is induced by the addition of the proton, one bond length increasing while the other one decreases all along the reaction path.

The (*R*) and (*S*) pathways for this reaction show only a small energy difference in the transition state (Scheme 3), as would be expected from the experimentally observed *ee*

Table 3. AM1-calculated (*R*) and (*S*) transition states

Configuration	Imaginary frequency [cm^{-1}] (AM1)	C(11)−C(15)	C(11)−H(1)	H(1)−O(4)	ΔH(AM1) [kcal/mol]	ΔH(BS1//AM1) [kcal/mol]
(*S*)	−445.0	1.94	2.95	2.34	0.0	0.0
(*R*)	−413.4	1.96	3.02	3.56	+4.5	+3.7

Table 4. Bond lengths [Å] corresponding to possible O−H interactions

	O(4)−H(1)	O(4)−H(2)	O(4)−H(3)	O(3)−H(4)
(*S*) Enantiomer	2.34	2.22	2.50	2.46
(*R*) Enantiomer	3.04	2.18	2.26	3.92

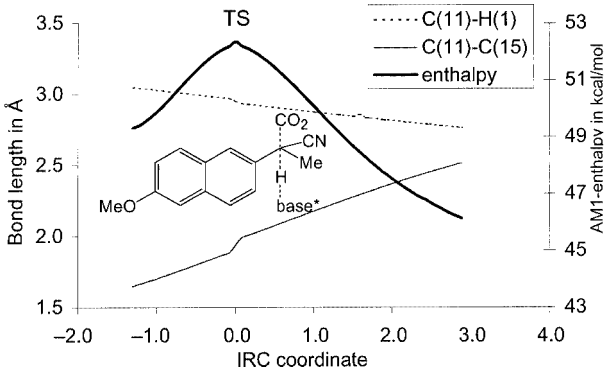

Figure 7. IRC profile and changes in bond length for the (*S*) transition state

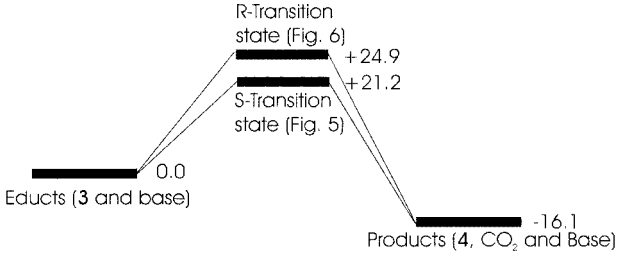

Scheme 3. DFT profile of the two pathways (B3LYP/6-31G*//AM1; kcal/mol)

values. The DFT energies for the starting materials, the two transition states, and the products were calculated with Becke3LYP/6-31G(d)//AM1.

The decarboxylation of the (*S*) enantiomeric starting material is an inversion. Formally, however, as the substituent with the highest priority according to the CIP rules is replaced by a substituent with the lowest priority, the relative configuration in the product remains (*S*).

Unfortunately, the solvent calculations on the concerted pathway could not be completed due to technical problems. We expect that a solvent model would also give a moderate decrease in the calculated energies in this case. Keeping in mind that the calculated energy values for the "solvated" two-step mechanism are still higher than those of the "non-solvated" concerted pathway, we propose that the reaction follows the concerted mechanism.

Conclusion

From a combined DFT and DFT/AM1 study, we propose that the asymmetric decarboxylation reaction in the synthesis of Naproxen proceeds through a concerted transition state and not by a two-step reaction as originally reported.

The calculated energy profile for the proposed sequence of deprotonation of the acid, decarboxylation, and reprotonation of the intermediate ketenimine anion was several kcal/mol less favorable (by gas-phase and solvent calculation) than the concerted reaction, which required a gas-phase activation enthalpy of 21.2 kcal/mol.

The key interactions in the transition state are C−H···O and N−H···O "bonds", which stabilize the (*S*) transition state more than the corresponding (*R*) transition state.

Acknowledgments

We are indebted to Professor W. A. Herrmann for his generous and continuous support of our work. We are also grateful to the Leibniz-Rechenzentrum Muenchen for providing the necessary computer time.

[1] C. Giordano, M. Villa, S. Panossian, in *Chirality in Industry* (Eds.: A. N. Collins, G. N. Sheldrake, J. Crosby), Wiley, New York, **1992**, p. 303.
[2] C. Giordano, G. Castaldi, S. Cavicchioli, M. Villa, *Tetrahedron* **1989**, *45*, 4243−4252.
[3] T. V. RajanBabu, A. L. Casalnuovo, *J. Am. Chem. Soc.* **1992**, *114*, 6265−6266.
[4] A. L. Casalnuovo, T. V. RajanBabu, T. A. Ayers, T. H. Warren, *J. Am. Chem. Soc.* **1994**, *116*, 9869−9882.
[5] Q. M. Gu, C. S. Chen, C. J. Sih, *Tetrahedron Lett.* **1986**, *27*, 1763−1766.
[6] F. Effenberger, B. W. Graef, S. Osswald, *Tetrahedron: Asymmetry* **1997**, *8*, 2749−2755.
[7] M. Garcia, C. del Campo, E. F. Llama, J. M. Sanchez-Montero, V. Sinisterra, *Tetrahedron* **1993**, *49*, 8433−8440.
[8] T. Ohta, H. Takaya, M. Kitamura, K. Nagai, R. Noyori, *J. Org. Chem.* **1987**, *52*, 3174−3176.
[9] T. Ohta, H. Takaya, R. Noyori, *Inorg. Chem.* **1988**, *27*, 566−569.
[10] R. D. Larsen, E. G. Corley, P. Davis, P. J. Reider, E. J. J. Grabowski, *J. Am. Chem. Soc.* **1989**, *111*, 7650−7651.
[11] C. E. Cannizzaro, T. Strassner, K. N. Houk, *J. Am. Chem. Soc.* **2001**, *123*, 2668−2669.
[12] H. Brunner, P. Schmidt, *Eur. J. Org. Chem.* **2000**, 2119−2133.
[13] H. Brunner, P. Schmidt, *Z. Naturforsch., B: Chem. Sci.* **2000**, *55*, 369−372.

[14] H. Brunner, M. Kurzwart, *Monatsh. Chem.* **1992**, *123*, 121−128.
[15] H. Brunner, J. Mueller, J. Spitzer, *Monatsh. Chem.* **1996**, *127*, 845−858.
[16] O. Toussaint, P. Capdevielle, M. Maumy, *Tetrahedron Lett.* **1987**, *28*, 539−542.
[17] A. D. Becke, *J. Chem. Phys.* **1992**, *97*, 9173−9177.
[18] A. D. Becke, *J. Chem. Phys.* **1993**, *98*, 5648−5652.
[19] A. D. Becke, *J. Chem. Phys.* **1993**, *98*, 1372−1377.
[20] M. J. Frisch, G. W. Trucks, H. B. Schlegel, G. E. Scuseria, M. A. Robb, J. R. Cheeseman, V. G. Zakrzewski, J. A. Montgomery Jr., R. E. Stratmann, J. C. Burant, S. Dapprich, J. M. Millam, A. D. Daniels, K. N. Kudin, M. C. Strain, O. Farkas, J. Tomasi, V. Barone, M. Cossi, R. Cammi, B. Mennucci, C. Pomelli, C. Adamo, S. Clifford, J. Ochterski, G. A. Petersson, P. Y. Ayala, Q. Cui, K. Morokuma, D. K. Malick, A. D. Rabuck, K. Raghavachari, J. B. Foresman, J. Cioslowski, J. V. Ortiz, B. B. Stefanov, G. Liu, A. Liashenko, P. Piskorz, I. Komaromi, R. Gomperts, R. L. Martin, D. J. Fox, T. Keith, M. A. Al-Laham, C. Y. Peng, A. Nanayakkara, C. Gonzalez, M. Challacombe, P. M. W. Gill, B. Johnson, W. Chen, M. W. Wong, J. L. Andres, C. Gonzalez, M. Head-Gordon, E. S. Replogle, J. A. Pople, *GAUSSIAN-98*, Gaussian, Inc., Pittsburgh, PA, **1998**.
[21] M. J. S. Dewar, E. G. Zoebisch, E. F. Healy, J. J. P. Stewart, *J. Am. Chem. Soc.* **1985**, *107*, 3902−3909.
[22] L. Onsager, *J. Am. Chem. Soc.* **1936**, *58*, 1486−1493.
[23] J. G. Kirkwood, *J. Chem. Phys.* **1934**, *2*, 351−361.
[24] M. W. Wong, M. J. Frisch, K. B. Wiberg, *J. Am. Chem. Soc.* **1991**, *113*, 4776−4782.
[25] M. W. Wong, K. B. Wiberg, M. Frisch, *J. Chem. Phys.* **1991**, *95*, 8991−8998.
[26] M. W. Wong, K. B. Wiberg, M. J. Frisch, *J. Am. Chem. Soc.* **1992**, *114*, 1645−1652.
[27] M. W. Wong, K. B. Wiberg, M. J. Frisch, *J. Am. Chem. Soc.* **1992**, *114*, 523−529.
[28] Starting with the quinuclidine core only, we added the substituents and aromatic rings step by step. In every step we first searched for the transition state and verified it by a frequency calculation. We then added groups while keeping the "transition-state" bond length frozen. After full optimization we used the resulting geometry for a new transition-state search. We followed the Eigenvector for the loss of carbon dioxide and confirmed the nature of the new stationary point again by a frequency calculation. This procedure was repeated until the full system could be optimized.

Received November 19, 2001
[O01551]